ELSEVIER

Superlattices and Microstructures 35 (2004) 629–643

Superlattices and Microstructures

www.elsevier.com/locate/superlattices

Discrete velocity modelling of gaseous mixture flows in MEMS

S. Naris[a], D. Valougeorgis[a,*], F. Sharipov[b], D. Kalempa[b]

[a] *Department of Mechanical and Industrial Engineering, University of Thessaly, Pedion Areos, Volos 38333, Greece*

[b] *Departamento de Física, Universidade Federal do Paraná, Caixa Postal 19044, 81531-990 Curitiba, Brazil*

Received 26 May 2003; received in revised form 12 January 2004; accepted 9 February 2004

Abstract

The need of developing advanced micro-electro-mechanical systems (MEMS) has motivated the study of fluid-thermal flows in devices with micro-scale geometries. In many MEMS applications the Knudsen number varies in the range from 10^{-2} to 10^{2}. This flow regime can be treated neither as a continuum nor as a free molecular flow. In order to describe these flows it is necessary to implement the Boltzmann equation (BE) or simplified kinetic model equations.

The aim of the present work is to propose an efficient methodology for solving internal flows of binary gaseous mixtures in rectangular channels due to small pressure gradients over the whole range of the Knudsen number. The complicated collision integral term of the BE is substituted by the kinetic model proposed by McCormack for gaseous mixtures. The discrete velocity method is implemented to solve in an iterative manner the system of the kinetic equations. Even more the required computational effort is significantly reduced, by accelerating the convergence rate of the iteration scheme. This is achieved by formulating a set of moment equations, which are solved jointly with the transport equations.

The velocity profiles and the flow rates of three different binary mixtures (He–Ar, Ne–Ar and He–Xe) in 2D micro-channels of various height to width ratios are calculated. The whole formulation becomes very efficient and can be implemented as an alternative methodology to the classical method of solving the Navier–Stokes equations with slip boundary conditions, which in any case is restricted by the hydrodynamic regime.

Keywords: Micro-fluidics; Rarefied gases; Mixtures; Internal flows

* Corresponding author. Tel.: +30-2421-074058; fax: +30-2421-074059.
E-mail address: diva@mie.uth.gr (D. Valougeorgis).

0749-6036/$ - see front matter © 2004 Elsevier Ltd. All rights reserved.
doi:10.1016/j.spmi.2004.02.025

1. Introduction

The development of technologies in micro-electro-mechanical systems (MEMS) has motivated the study of fluid flows in devices with micro or meso-scale geometries [1]. In MEMS the Knudsen number, which is defined as the ratio of the mean free path λ of the fluid molecules to a typical geometric dimension H of the device ($Kn = \lambda/H$), varies in the range from 10^{-2} to 10^{2}. In this range known as the transition regime, the continuum hypothesis, which is the basic one for the Navier–Stokes equations breaks down and the implementation of the Boltzmann equation (BE) or simplified kinetic equations is required [2]. In general, these equations are more difficult to solve than the hydrodynamic equations. For that reason in many occasions the continuum equations are applied even in the transition regime coupled with appropriate slip boundary conditions [3]. It is evident however, that approaches based on kinetic theory are more suitable to handle this type of problem, since the whole range of gas rarefaction can be studied in a unique manner. Nowadays, it is possible to solve directly the model kinetic equation and the BE itself due to the availability of parallel high speed computers and due to the significant advancement of numerical methods in kinetic theory made during the last years. A number of complex problems concerning multi-dimensional flows of rarefied gases have been solved in an accurate and computationally efficient manner [4, 5]. This outcome explains the renewed interest in kinetic approaches and makes researchers optimistic for solving continuum problems based on kinetic type (mesoscopic) approaches [6].

The aim of the present work is to provide an efficient methodology for solving internal flows of binary gaseous mixtures through rectangular channels, over the whole range of the Knudsen number. The corresponding single gas problem has been extensively studied over the last forty years in 1D [2, 7] and recently in 2D [8, 9]. In spite of the great practical importance of the internal flows of gaseous mixtures there are very few articles in the literature concerning this topic. Practically all of them deal with plane and axi-symmetric geometric configurations [10–16].

In the present work we consider a flow of binary gaseous mixture through 2D channels caused by a small longitudinal pressure gradient. The McCormack kinetic model [17] is applied to substitute the complicated collision integral of the BE. This model satisfies the conservation laws, the H-theorem and provides the correct expressions of all transport coefficients. The discrete velocity method (DVM) [7] is applied to solve the coupled kinetic equations in an iterative manner. The DVM is simple, easy to implement and highly parallelized. However, at the continuum limit, which is of practical interest in MEMS, its convergence rate becomes very slow. An optimization of the DVM, based on the idea of using the continuum solution in numerical calculations of rarefied gas flows has been proposed in [18] and as a result the required number of spatial grid points has been reduced significantly. The required number of the iterations however, remains high. The methodology used in the present work allows us to reduce significantly the number of the iterations introducing a set of diffusion synthetic equations by taking moments of the kinetic equations [19]. Then the kinetic equations and their moments are solved jointly and the convergence rate of the scheme improves dramatically [9]. As a result the proposed kinetic type approach becomes more attractive and promising for multidimensional problems with complex boundaries. Numerical results for the flow rates

and the velocity profiles are provided for the binary mixtures of He–Ar, Ne–Ar and He–Xe in rectangular channels with various height to width (aspect) ratios, for the whole range of gas rarefaction. Finally, the efficiency of the new accelerated scheme is compared with the typical DVM by estimating the required computational time of the two schemes imposing the same convergence criteria.

2. Statement of the problem and input equations

Consider a flow of a binary gaseous mixture through a long micro-channel of a constant rectangular cross section. The transverse directions are along the x' and y' axis, with $-\frac{W}{2} \leq x' \leq \frac{W}{2}$ and $-\frac{H}{2} \leq y' \leq \frac{H}{2}$, while the ratio of the height H to the width W is the aspect ratio. Without loss of generality the height is taken less than or equal to the width of the channel ($H \leq W$). The flow in the longitudinal direction z is caused by a small pressure gradient

$$\upsilon = \frac{H}{P}\frac{\partial P}{\partial z'} \qquad |\upsilon| \ll 1 \tag{1}$$

where P is the pressure of the mixture in a given cross section. The end effects are neglected by assuming the channel length L to be much longer than its width W. Thus, the flow may be considered as fully developed and we solve only for the longitudinal component of the hydrodynamic (bulk) velocity vector.

The molar concentration of each species in the mixture is

$$C_\alpha = \frac{n_\alpha}{n_1 + n_2}, \qquad \alpha = 1, 2 \tag{2}$$

where n_α is the equilibrium number density of species α and $C_1 + C_2 = 1$. Here, we choose to denote $C_1 = C$ and consequently $C_2 = 1 - C$. Then the mean molecular mass of the mixture is defined as

$$m = Cm_1 + (1 - C)m_2 \tag{3}$$

where m_α is the molecular mass of species α. The rarefaction parameter is given by

$$\delta = \frac{HP}{\mu}\left(\frac{m}{2kT}\right)^{1/2} \tag{4}$$

where μ is the viscosity of the mixture, T is its temperature and k is the Boltzmann constant. Considering that the viscosity is proportional to the molecular mean free path λ, one can see that the rarefaction parameter δ is proportional to the inverse Knudsen number defined as $Kn = \lambda/H$.

For the further derivations it is convenient to introduce the dimensionless space variables

$$x = \frac{x'}{H}, \qquad y = \frac{y'}{H}, \qquad z = \frac{z'}{H}. \tag{5}$$

The distribution function of each species α is linearized as

$$f_\alpha(x, y, z, \mathbf{c}_\alpha) = f_\alpha^{(0)}(\mathbf{c}_\alpha)[1 + \upsilon z + h_\alpha(x, y, \mathbf{c}_\alpha)] \tag{6}$$

where $\mathbf{c}_\alpha = (c_{\alpha x}, c_{\alpha y}, c_{\alpha z})$ is the dimensionless molecular velocity, $h_\alpha(x, y, \mathbf{c}_\alpha)$ is the perturbation function and

$$f_\alpha^{(0)} = n_\alpha \left(\frac{m_\alpha}{2\pi kT}\right)^{3/2} \mathrm{e}^{-c_\alpha^2} \tag{7}$$

is the absolute Maxwellian equilibrium function. Then the system of the kinetic Boltzmann equations for the unknown perturbation functions, in dimensionless form, reads [14]

$$c_{\alpha x}\frac{\partial h_\alpha}{\partial x} + c_{\alpha y}\frac{\partial h_\alpha}{\partial y} = d_\alpha \sum_{\beta=1}^{2} L_{\alpha\beta} h_\alpha - c_{\alpha z}, \qquad \alpha = 1, 2. \tag{8}$$

The complicated linearized collision term is substituted, by the kinetic model proposed by McCormack [17]. For the isothermal problem under consideration the density and temperature departures from their corresponding equilibrium values are zero and the McCormack linearized collision term becomes [14]

$$\begin{aligned} L_{\alpha\beta}h_\alpha = {} & -\gamma_{\alpha\beta}h_\alpha + 2\sqrt{\frac{m_\alpha}{m}}\left[\gamma_{\alpha\beta}u_\alpha - \nu_{\alpha\beta}^{(1)}(u_\alpha - u_\beta) - \frac{1}{2}\nu_{\alpha\beta}^{(2)}\left(q_\alpha - \frac{m_\alpha}{m_\beta}q_\beta\right)\right]c_{\alpha z} \\ & + 4[(\gamma_{\alpha\beta} - \nu_{\alpha\beta}^{(3)})\Pi_{\alpha xz} + \nu_{\alpha\beta}^{(4)}\Pi_{\beta xz}]c_{\alpha z}c_{\alpha x} \\ & + 4[(\gamma_{\alpha\beta} - \nu_{\alpha\beta}^{(3)})\Pi_{\alpha yz} + \nu_{\alpha\beta}^{(4)}\Pi_{\beta yz}]c_{\alpha z}c_{\alpha y} \\ & + \frac{4}{5}\sqrt{\frac{m_\alpha}{m}}\left[(\gamma_{\alpha\beta} - \nu_{\alpha\beta}^{(5)})q_\alpha + \nu_{\alpha\beta}^{(6)}\sqrt{\frac{m_\beta}{m_\alpha}}q_\beta - \frac{5}{4}\nu_{\alpha\beta}^{(2)}(u_\alpha - u_\beta)\right]c_{\alpha z} \\ & \times \left(c_\alpha^2 - \frac{5}{2}\right), \end{aligned}$$

where

$$u_\alpha(x, y) = \frac{1}{\pi^{3/2}}\left(\frac{m}{m_\alpha}\right)^{1/2}\int h_\alpha(x, y, \mathbf{c}_\alpha)c_{\alpha z}\mathrm{e}^{-c_\alpha^2}\mathrm{d}\mathbf{c}_\alpha \tag{9}$$

$$q_\alpha(x, y) = \frac{1}{\pi^{3/2}}\left(\frac{m}{m_\alpha}\right)^{1/2}\int h_\alpha(x, y, \mathbf{c}_\alpha)c_{\alpha z}\left(c_\alpha^2 - \frac{5}{2}\right)\mathrm{e}^{-c_\alpha^2}\mathrm{d}\mathbf{c}_\alpha \tag{10}$$

and

$$\Pi_{\alpha iz}(x, y) = \frac{1}{\pi^{3/2}}\int h_\alpha(x, y, \mathbf{c}_\alpha)c_{\alpha z}c_{\alpha i}\mathrm{e}^{-c_\alpha^2}\mathrm{d}\mathbf{c}_\alpha, \qquad i = x, y. \tag{11}$$

These moments of the perturbation function are related to the hydrodynamic velocity, the heat flux and the shear stress tensor of each species, respectively. It is worth noting that in the transition regime, even under the isothermal conditions, there is a heat flux due to the pressure gradient, which disappears in the continuum limit. This phenomenon is known as the mechanocaloric effect [20]. The expressions of the parameters $\gamma_{\alpha\beta}$ and $\nu_{\alpha\beta}^{(i)}$ are explicitly given in the Appendix. Finally, using Eq. (4) and the expressions of the Appendix, it is easily seen that

$$d_\alpha = \delta\left[\frac{C}{\gamma_1} + \frac{1 - C}{\gamma_2}\right]\sqrt{\frac{m_\alpha}{m}}, \tag{12}$$

where the collision frequencies $\gamma_1 = \gamma_{11} + \gamma_{12}$ and $\gamma_2 = \gamma_{21} + \gamma_{22}$.

Our objective here is to efficiently solve Eq. (8) for the whole range of rarefaction, based on the proposed accelerated version of the DVM. In order to demonstrate the methodology in a more clear and precise manner, we choose to implement, due to their simplicity and clarity, the diffuse Maxwell boundary conditions. It is noted however, that the present formulation can be extended to include more complicated and advanced conditions at the walls, such as the diffuse-specular boundary conditions and the Cercignani–Lampis model.

The dimensionless quantities of our interest include the mean velocity of the mixture, which is a function of the two transverse directions and the volumetric flow rate given by

$$w(x, y) = Cu_1(x, y) + (1 - C)u_2(x, y) \tag{13}$$

and

$$J = CJ_1 + (1 - C)J_2 \tag{14}$$

respectively, where the dimensionless flow rate of each species is

$$J_\alpha = -2\frac{H}{W}\int_{-W/2H}^{W/2H}\int_{-1/2}^{1/2} u_\alpha(x, y)\,\mathrm{d}x\,\mathrm{d}y, \qquad \alpha = 1, 2. \tag{15}$$

In Section 5, numerical results are presented for the volumetric flow rate J of the mixture and the hydrodynamic (bulk) velocities $u_\alpha(x, y)$ for three different binary gas mixtures over a wide range of the rarefaction parameter δ and for various aspect ratios W/H, on the basis of the kinetic equations (8).

3. The discrete velocity method

The well known DVM has been used extensively over recent years to solve the BE or model kinetic equations [7]. So, its description is omitted here. Only the key issues related to the present formulation are presented for completeness and clarity.

Since the flow is considered as fully developed in the longitudinal direction z, the $c_{\alpha z}$ component of the molecular velocity is eliminated, by introducing the reduced functions

$$\Phi_\alpha(x, y, c_{\alpha x}, c_{\alpha y}) = \frac{1}{\sqrt{\pi}}\int h_\alpha(x, y, \mathbf{c}_\alpha)c_{\alpha z}\mathrm{e}^{-c_{\alpha z}^2}\mathrm{d}c_{\alpha z} \tag{16}$$

$$\Psi_\alpha(x, y, c_{\alpha x}, c_{\alpha y}) = \frac{1}{\sqrt{\pi}}\int h_\alpha(x, y, \mathbf{c}_\alpha)c_{\alpha z}^3\mathrm{e}^{-c_{\alpha z}^2}\mathrm{d}c_{\alpha z}. \tag{17}$$

Eq. (8) is multiplied by $\frac{1}{\sqrt{\pi}}c_{\alpha z}\mathrm{e}^{-c_{\alpha z}^2}$ and $\frac{1}{\sqrt{\pi}}c_{\alpha z}^3\mathrm{e}^{-c_{\alpha z}^2}$ successively and the resulting equations are integrated with respect to $c_{\alpha z}$, to obtain

$$c_{\alpha x}\frac{\partial \Phi_\alpha}{\partial x} + c_{\alpha y}\frac{\partial \Phi_\alpha}{\partial y} + \gamma_\alpha d_\alpha \Phi_\alpha = -\frac{1}{2} + d_\alpha \sum_{\beta=1}^{2}\left\{\sqrt{\frac{m_\alpha}{m}}\left[\gamma_{\alpha\beta}u_\alpha - \nu_{\alpha\beta}^{(1)}(u_\alpha - u_\beta) - \frac{1}{2}\nu_{\alpha\beta}^{(2)}\left(q_\alpha - \frac{m_\alpha}{m_\beta}q_\beta\right)\right]\right.$$

$$+ 2[(\gamma_{\alpha\beta} - \nu_{\alpha\beta}^{(3)})\Pi_{\alpha xz} + \nu_{\alpha\beta}^{(4)}\Pi_{\beta xz}]c_{\alpha x} + 2[(\gamma_{\alpha\beta} - \nu_{\alpha\beta}^{(3)})\Pi_{\alpha yz} + \nu_{\alpha\beta}^{(4)}\Pi_{\beta yz}]c_{\alpha y}$$
$$+ \frac{2}{5}\sqrt{\frac{m_\alpha}{m}}\left[(\gamma_{\alpha\beta} - \nu_{\alpha\beta}^{(5)})q_\alpha + \nu_{\alpha\beta}^{(6)}\sqrt{\frac{m_\beta}{m_\alpha}}q_\beta - \frac{5}{4}\nu_{\alpha\beta}^{(2)}(u_\alpha - u_\beta)\right]$$
$$\times (c_{\alpha x}^2 + c_{\alpha y}^2 - 1)\Bigg\} \tag{18}$$

and

$$c_{\alpha x}\frac{\partial \Psi_\alpha}{\partial x} + c_{\alpha y}\frac{\partial \Psi_\alpha}{\partial y} + \gamma_\alpha d_\alpha \Psi_\alpha$$
$$= -\frac{3}{4} + d_\alpha \sum_{\beta=1}^{2}\Bigg\{\frac{3}{2}\sqrt{\frac{m_\alpha}{m}}\left[\gamma_{\alpha\beta}u_\alpha - \nu_{\alpha\beta}^{(1)}(u_\alpha - u_\beta) - \frac{1}{2}\nu_{\alpha\beta}^{(2)}\left(q_\alpha - \frac{m_\alpha}{m_\beta}q_\beta\right)\right]$$
$$+ 3[(\gamma_{\alpha\beta} - \nu_{\alpha\beta}^{(3)})\Pi_{\alpha xz} + \nu_{\alpha\beta}^{(4)}\Pi_{\beta xz}]c_{\alpha x} + 3[(\gamma_{\alpha\beta} - \nu_{\alpha\beta}^{(3)})\Pi_{\alpha yz} + \nu_{\alpha\beta}^{(4)}\Pi_{\beta yz}]c_{\alpha y}$$
$$+ \frac{3}{5}\sqrt{\frac{m_\alpha}{m}}\left[(\gamma_{\alpha\beta} - \nu_{\alpha\beta}^{(5)})q_\alpha + \nu_{\alpha\beta}^{(6)}\sqrt{\frac{m_\beta}{m_\alpha}}q_\beta - \frac{5}{4}\nu_{\alpha\beta}^{(2)}(u_\alpha - u_\beta)\right]$$
$$\times (c_{\alpha x}^2 + c_{\alpha y}^2)\Bigg\}. \tag{19}$$

The quantities given by Eqs. (9)–(11), are now expressed via Φ_α and Ψ_α as

$$u_\alpha(x,y) = \frac{1}{\pi}\left(\frac{m}{m_\alpha}\right)^{1/2}\int_{-\infty}^{\infty}\int_{-\infty}^{\infty}\Phi_\alpha \mathrm{e}^{-c_{\alpha x}^2 - c_{\alpha y}^2}\,\mathrm{d}c_{\alpha x}\mathrm{d}c_{\alpha y} \tag{20}$$

$$q_\alpha(x,y) = \frac{1}{\pi}\left(\frac{m}{m_\alpha}\right)^{1/2}\int_{-\infty}^{\infty}\int_{-\infty}^{\infty}\left[\Psi_\alpha + \left(c_{\alpha x}^2 + c_{\alpha y}^2 - \frac{5}{2}\right)\Phi_\alpha\right]$$
$$\times \mathrm{e}^{-c_{\alpha x}^2 - c_{\alpha y}^2}\,\mathrm{d}c_{\alpha x}\mathrm{d}c_{\alpha y} \tag{21}$$

and

$$\Pi_{\alpha iz}(x,y) = \frac{1}{\pi}\int_{-\infty}^{\infty}\int_{-\infty}^{\infty}\Phi_\alpha c_{\alpha i}\mathrm{e}^{-c_{\alpha x}^2 - c_{\alpha y}^2}\,\mathrm{d}c_{\alpha x}\,\mathrm{d}c_{\alpha y}, \qquad i = x, y. \tag{22}$$

Eqs. (18)–(22) are discretized first in the velocity space $(c_{\alpha x}, c_{\alpha y})$ and then in the physical space (x, y). The roots of the Hermite polynomial of order N is chosen to define the set of discrete velocities for each component of the particle velocity $(c_{\alpha x}^k, c_{\alpha y}^l)$, $k, l = 1, 2, \ldots, N$, yielding a total number of N^2 discrete velocities. The discretization in the physical space is performed using the so-called diamond-difference scheme, which is a second order difference scheme [21]. The overall quantities at the right hand side of Eqs. (18) and (19) are estimated from Eqs. (20)–(22) using a double Gauss–Hermite quadrature scheme of order N. The iterative solution of the discretized version of Eqs. (18) and (19) is known as the DVM and it consists of the following steps:

(i) Assume u_α, $\Pi_{\alpha iz}$ and q_α and compute Φ_α and Ψ_α from Eqs. (18) and (19).

(ii) Estimate the new values of u_α, $\Pi_{\alpha iz}$ and q_α from Eqs. (20)–(22).

(iii) Go back to step (i) and use the updated values of u_α, $\Pi_{\alpha iz}$ and q_α to compute the new Φ_α and Ψ_α. The iterative procedure is ended when the imposed convergence criterion on the overall quantities is satisfied.

It is noted that by considering purely diffuse Maxwell boundary conditions [2] at the walls, the reduced functions Φ_α and Ψ_α are known and the algorithm is applied only in the interior nodes. It is easily deduced that the reduced functions at the four walls of the rectangular channel are:

$$\Phi_\alpha(x, -\tfrac{1}{2}, c_{\alpha x}, c_{\alpha y}) = \Psi_\alpha(x, -\tfrac{1}{2}, c_{\alpha x}, c_{\alpha y}) = 0, \quad c_{\alpha x} \in (-\infty, \infty), \quad c_{ay} \in [0, \infty) \tag{23}$$

$$\Phi_\alpha(x, +\tfrac{1}{2}, c_{\alpha x}, c_{\alpha y}) = \Psi_\alpha(x, +\tfrac{1}{2}, c_{\alpha x}, c_{\alpha y}) = 0, \quad c_{\alpha x} \in (-\infty, \infty), \quad c_{ay} \in (-\infty, 0] \tag{24}$$

$$\Phi_\alpha\left(-\frac{W}{2H}, y, c_{\alpha x}, c_{\alpha y}\right) = \Psi_\alpha\left(-\frac{W}{2H}, y, c_{\alpha x}, c_{\alpha y}\right) = 0, \quad c_{\alpha x} \in [0, \infty), \quad c_{ay} \in (-\infty, \infty) \tag{25}$$

$$\Phi_\alpha\left(+\frac{W}{2H}, y, c_{\alpha x}, c_{\alpha y}\right) = \Psi_\alpha\left(+\frac{W}{2H}, y, c_{\alpha x}, c_{\alpha y}\right) = 0, \quad c_{\alpha x} \in (-\infty, 0], \quad c_{ay} \in (-\infty, \infty). \tag{26}$$

Researchers implementing the DVM are well aware however, of its slow convergence particularly when the continuum regime is approached ($Kn \leq 0.1$ or $\delta \geq 10$). In these cases a large number of iterations is required and the calculations are amenable to accumulated round off error. Special attention is needed to sustain acceptable accuracy. Furthermore when 2D and 3D physical systems are examined, the computational effort and the CPU time are drastically increased. In the next section, this pitfall is circumvented, by introducing an accelerated version of the classical DVM.

4. Formulation of the accelerated scheme

In the field of neutron and radiative transport fast iterative algorithms have been well developed and effectively applied to speed up the iterative convergence of the discrete ordinate method in optically thick regions with low absorption and isotropic or anisotropic scattering [19]. These transport phenomena are modelled with linear integro-differential equations, which are similar to those implemented in kinetic theory of gases. Thus it is reasonable to expect that the acceleration schemes developed for the neutron and radiative transport can be extended with certain modifications to speed up the convergence rate of the DVM. Based on this idea in a recent work, a new fast iterative DVM has been introduced and its efficiency has been demonstrated by solving the flow of a single gas through a rectangular channel [9].

Here, this formulation is extended to the corresponding problem of a binary mixture. To carry this out first the Hermitian moments of Φ_α and Ψ_α are defined as

$$U^\alpha_{mn}(x, y) = \frac{1}{\pi}\left(\frac{m}{m_\alpha}\right)^{1/2} \int_{-\infty}^{\infty}\int_{-\infty}^{\infty} H_m(c_{\alpha x}) H_n(c_{\alpha y})\, \Phi_\alpha \mathrm{e}^{-c^2_{\alpha x} - c^2_{\alpha y}}\, \mathrm{d}c_{\alpha x}\, \mathrm{d}c_{\alpha y} \tag{27}$$

and

$$Q^{\alpha}_{mn}(x,y) = \frac{1}{\pi}\left(\frac{m}{m_\alpha}\right)^{1/2}\int_{-\infty}^{\infty}\int_{-\infty}^{\infty} H_m(c_{\alpha x})H_n(c_{\alpha y}) \times\left[\Psi_\alpha + \left(c^2_{\alpha x}+c^2_{\alpha y}-\frac{5}{2}\right)\Phi_\alpha\right]\mathrm{e}^{-c^2_{\alpha x}-c^2_{\alpha y}}\,\mathrm{d}c_{\alpha x}\,\mathrm{d}c_{\alpha y} \tag{28}$$

where H_m are the Hermite polynomials of the order m. Notice that by setting m and n equal to zero and/or one we have

$$U^{\alpha}_{00} = u_\alpha, \quad Q^{\alpha}_{00} = q_\alpha, \quad U^{\alpha}_{10} = 2\sqrt{\frac{m}{m_\alpha}}\Pi_{\alpha xz} \quad \text{and} \quad U^{\alpha}_{01} = 2\sqrt{\frac{m}{m_\alpha}}\Pi_{\alpha yz}. \tag{29}$$

Eqs. (18) and (19) are multiplied by $\frac{1}{\sqrt{\pi}}\sqrt{\frac{m}{m_\alpha}}\mathrm{e}^{-c^2_{\alpha x}-c^2_{\alpha x}}$ and then the resulting equations are multiplied successively by $H_0(c_{ax})H_0(c_{ay})$, $H_1(c_{ax})H_0(c_{ay})$ and $H_0(c_{ax})H_1(c_{ay})$. After a double integration with respect to $c_{\alpha x}$ and $c_{\alpha y}$ these equations yield three moment equations for each transport equation. The moment equations are combined appropriately and after some mathematical manipulation the following four synthetic moment equations are obtained:

$$\begin{aligned}
&\partial_{xx}U^{\alpha}_{00} + \partial_{yy}U^{\alpha}_{00} - 2d^2_\alpha(\nu^{(3)}_{\alpha\alpha} + \nu^{(3)}_{\alpha\beta} - \nu^{(4)}_{\alpha\alpha}) \\
&\quad\times\left[\nu^{(1)}_{\alpha\beta}(U^{\alpha}_{00}-U^{\beta}_{00}) + \frac{\nu^{(2)}_{\alpha\beta}}{2}\left(Q^{\alpha}_{00}-\frac{m_\alpha}{m_\beta}Q^{\beta}_{00}\right)\right] + 2d_\alpha d_\beta\sqrt{\frac{m_\beta}{m_\alpha}}\nu^{(4)}_{\alpha\beta} \\
&\quad\times\left[\nu^{(1)}_{\alpha\beta}(U^{\beta}_{00}-U^{\alpha}_{00}) + \frac{\nu^{(2)}_{\alpha\beta}}{2}\left(Q^{\beta}_{00}-\frac{m_\beta}{m_\alpha}Q^{\alpha}_{00}\right)\right] \\
&\quad= -\frac{1}{2}\partial_{xx}U^{\alpha}_{20} - \frac{1}{2}\partial_{yy}U^{\alpha}_{02} - \partial_{xy}U^{\alpha}_{11} + d_\alpha\sqrt{\frac{m}{m_\alpha}}[\nu^{(3)}_{\alpha\alpha} + \nu^{(3)}_{\alpha\beta} - \nu^{(4)}_{\alpha\alpha} - \nu^{(4)}_{\alpha\beta}]
\end{aligned} \tag{30}$$

$$\begin{aligned}
&\partial_{xx}Q^{\alpha}_{00} + \partial_{yy}Q^{\alpha}_{00} + 2d^2_\alpha\left[-(\nu^{(5)}_{\alpha\alpha} + \nu^{(5)}_{\alpha\beta} - \nu^{(6)}_{\alpha\alpha})Q^{\alpha}_{00} + \sqrt{\frac{m_\beta}{m_\alpha}}\nu^{(6)}_{\alpha\beta}Q^{\beta}_{00}\right. \\
&\quad\left.-\frac{5}{4}\nu^{(2)}_{\alpha\beta}(U^{\alpha}_{00}-U^{\beta}_{00})\right] + 2d^2_\alpha(\gamma_\alpha - \nu^{(3)}_{\alpha\alpha} - \nu^{(3)}_{\alpha\beta} + \nu^{(4)}_{\alpha\alpha}) \\
&\quad\times\left[\nu^{(1)}_{\alpha\beta}(U^{\alpha}_{00}-U^{\beta}_{00}) + \frac{\nu^{(2)}_{\alpha\beta}}{2}\left(Q^{\alpha}_{00}-\frac{m_\alpha}{m_\beta}Q^{\beta}_{00}\right)\right] + 2d_\alpha d_\beta\sqrt{\frac{m_\beta}{m_\alpha}}\nu^{(4)}_{\alpha\beta} \\
&\quad\times\left[\nu^{(1)}_{\alpha\beta}(U^{\beta}_{00}-U^{\alpha}_{00}) + \frac{\nu^{(2)}_{\alpha\beta}}{2}\left(Q^{\beta}_{00}-\frac{m_\beta}{m_\alpha}Q^{\alpha}_{00}\right)\right] \\
&\quad= -\frac{1}{2}\partial_{xx}Q^{\alpha}_{20} - \frac{1}{2}\partial_{yy}Q^{\alpha}_{02} - \partial_{xy}Q^{\alpha}_{11} - d_\alpha\sqrt{\frac{m}{m_\alpha}} \\
&\quad\times(\gamma_\alpha - \nu^{(3)}_{\alpha\alpha} - \nu^{(3)}_{\alpha\beta} + \nu^{(4)}_{\alpha\alpha} + \nu^{(4)}_{\alpha\beta})
\end{aligned} \tag{31}$$

with $\alpha, \beta = 1, 2$ and $\alpha \neq \beta$.

The above four equations are the acceleration equations. It is noted however, that only the zeroth moments of Φ_α and Ψ_α are accelerated, while the second moments at the right hand side of the above equations are estimated from Eqs. (27) and (28). Eqs. (30) and (31)

are coupled with the transport equations (18) and (19) and they are solved in an iterative manner. More specifically the accelerated DVM is consisting of the following steps:

(i) Assume U^{α}_{00}, Q^{α}_{00}, U^{α}_{10} and U^{α}_{01} and compute Φ_{α} and Ψ_{α} from Eqs. (18) and (19).
(ii) Estimate the second moments U^{α}_{20}, U^{α}_{11}, U^{α}_{02}, Q^{α}_{20}, Q^{α}_{11}, Q^{α}_{02}, which are not accelerated from Eqs. (27) and (28).
(iii) Solve the system of differential equations (30) and (31) and find the new values of U^{α}_{00} and Q^{α}_{00}.
(iv) Go back to step (i) and use the accelerated values of U^{α}_{00} and Q^{α}_{00} to compute the new Φ_{α} and Ψ_{α}. The iterative procedure is ended when the imposed convergence criterion on the overall quantities is satisfied.

Various acceleration schemes may be defined depending upon the number of accelerated moments. Following the terminology defined in the field of neutron transport theory [19], since the implemented acceleration equations look like diffusion type equations the present acceleration scheme is called the "diffusion synthetic acceleration (DSA)" scheme. It is obvious that the DSA scheme requires a greater computational effort per iteration than the typical DVM. However, as it is shown in the next section the DSA needs a much smaller number of iterations and consequently the total computational time is significantly reduced.

5. Results

The numerical results presented here, have been performed by the DSA algorithm. To test the accuracy of the accelerated code in some cases the typical DVM has also been implemented. For all cases tested, imposing identical velocity and space discretization schemes and the same convergence criteria, the corresponding results of the two schemes agree to each other up to at least three significant figures. In addition, by taking particles of the two species of equal molecular mass and diameter the binary gas problem is reduced to the corresponding two-dimensional single gas problem, described by the S kinetic model [8, 9]. Again, the results are in an excellent agreement.

The calculations have been carried out over the wide range of the rarefied parameter δ from 10^{-3} up to 40^2, with the aspect ratio H/W equal to 1, 0.1 and 0.05. The gaseous mixtures of Ne–Ar, He–Ar and He–Xe have been examined with a molar concentration $C = 0.5$. The molecular masses are $m_{\mathrm{He}} = 4.0026$, $m_{\mathrm{Ne}} = 20.183$, $m_{\mathrm{Ar}} = 39.948$ and $m_{\mathrm{Xe}} = 131.30$ in atomic units.

To calculate the quantities $\nu^{(i)}_{\alpha b}$ an intermolecular interaction law must be assumed. As was shown in [22] the momentum transfer phenomenon is not sensitive to this interaction law. So, in our calculations the hard sphere molecular model is considered. To carry out the calculations only the molecular diameter ratios are needed, and they are calculated from the experimental data on the viscosities of each species [23] at the temperature $T = 300$ K. Finally, the ratios of the diameters have been found equal to 1.406, 1.665 and 2.226 for Ne–Ar, He–Ar and He–Xe respectively.

All presented results are based on a 128 point Gauss–Hermite quadrature scheme with respect to each velocity component $(c_{\alpha x}, c_{\alpha y})$, while the grids in the physical space are taken 31×31 for $H/W = 1$ and 31×61 for $H/W = 0.1$ and 0.05. Based on the

Table 1
Dimensionless volumetric flow rate J for various δ and H/W for the Ne–Ar mixture

δ	J		
	$H/W = 1$	$H/W = 0.1$	$H/W = 0.05$
0.001	0.8738	2.063	2.447
0.01	0.8648	1.990	2.317
0.1	0.8298	1.747	1.919
1	0.8009	1.484	1.541
10	1.340	2.638	2.721
40	3.413	7.25	7.49

Table 2
Dimensionless volumetric flow rate J for various δ and H/W for the He–Ar mixture

δ	J		
	$H/W = 1$	$H/W = 0.1$	$H/W = 0.05$
0.001	1.291	3.049	3.620
0.01	1.278	2.947	3.438
0.1	1.219	2.563	2.824
1	1.092	1.954	2.028
10	1.464	2.817	2.904
40	3.494	7.38	7.62

Table 3
Dimensionless volumetric flow rate J for various δ and H/W for the He–Xe mixture

δ	J		
	$H/W = 1$	$H/W = 0.1$	$H/W = 0.05$
0.001	2.021	4.777	5.674
0.01	2.002	4.629	5.412
0.1	1.906	4.020	4.449
1	1.619	2.806	2.911
10	1.669	3.082	3.173
40	3.595	7.53	7.77

aforementioned discretization, the present numerical results have converged to ± 1 to the last significant figure given here.

The dimensionless flow rate J is given in Tables 1–3 for the three gaseous mixtures under investigation. The variation of the flow rate with respect to δ and H/W is similar to that for a single gas [8]. For all three mixtures, it has a minimum at $\delta \sim 1$ and it increases by increasing δ. For $H/W = 1$ the minimum is shallow, while for the other two smaller aspect ratios it is deep.

In Figs. 1–3 some typical velocity profiles $u_\alpha(x, 0)$, in the case of the square channel ($H/W = 1$) are plotted for the gaseous mixtures of Ne–Ar, He–Ar and He–Xe respectively. It can be seen that near the hydrodymanic regime ($\delta = 40$) the profiles of

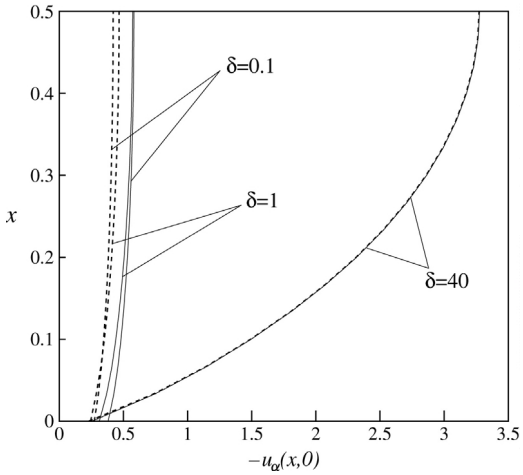

Fig. 1. Velocity profiles of each species $u_\alpha(x, 0)$ for the Ne–Ar mixture for various values of δ (solid line—Ne, dashed line—Ar).

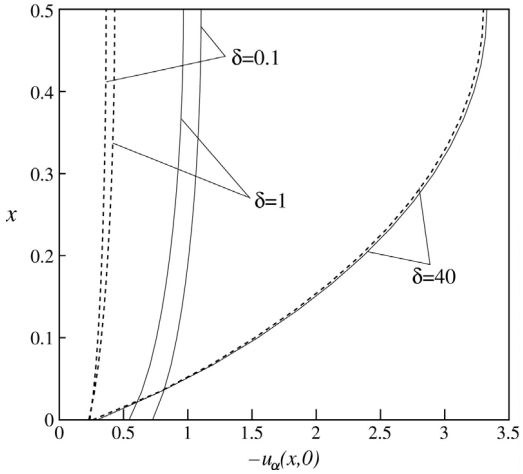

Fig. 2. Velocity profiles of each species $u_\alpha(x, 0)$ for the He–Ar mixture for various values of δ (solid line—He, dashed line—Ar).

both species are parabolic and equal to each other, which corresponds to the solution of the Navier–Stokes equations with slip boundary conditions. For the free molecular and the transition regimes ($\delta = 1$ and 0.1) the velocities of each species are different with the lighter component having the higher velocity.

A comparison between the DVM and the proposed DSA scheme in terms of required number of iterations and total CPU time is demonstrated in Figs. 4 and 5, respectively. The required number of iterations to satisfy the convergence criterion in the computed results

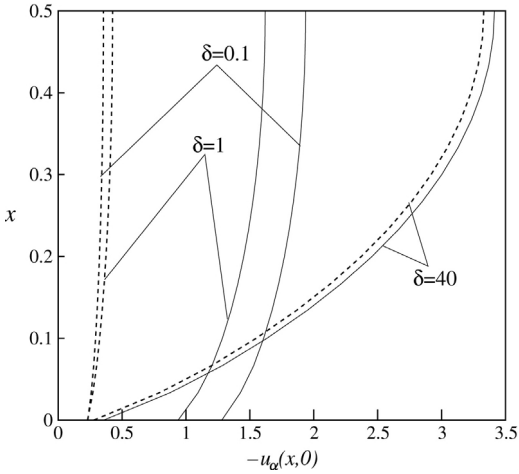

Fig. 3. Velocity profiles of each species $u_\alpha(x, 0)$ for the He–Xe mixture for various values of δ (solid line—He, dashed line—Xe).

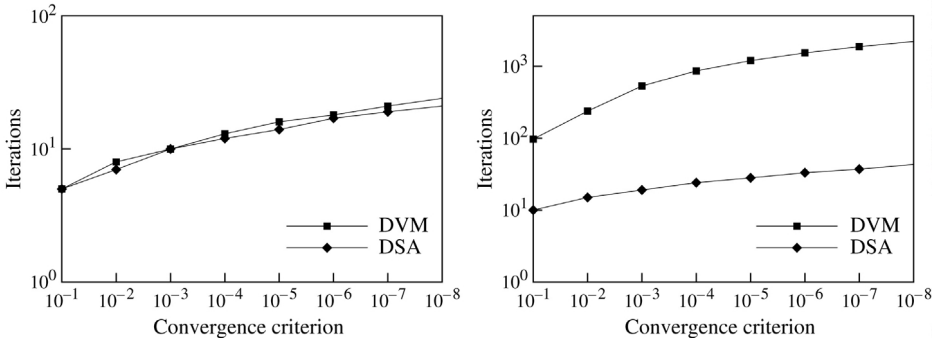

Fig. 4. Comparison between the DVM and the DSA method in terms of the number of iterations to satisfy the convergence criterion for $\delta = 1$ (left) and $\delta = 40$ (right).

is plotted as a function of the convergence criterion in Fig. 4. The results are presented for $\delta = 1$ and 40 and for the case of the square channel. It can be seen that for $\delta = 1$ the number of required iterations is very small and there is no benefit in using the DSA scheme. For $\delta = 40$ however, the required number of iterations for the typical DVM is significantly increased, while for the DSA scheme it remains small. More specifically, for $\delta = 40$ and for a relative convergence criterion of 10^{-5} the required iterations for the DSA scheme are reduced roughly by a factor of 100. It is also noted that the required number of iterations for the acceleration scheme remains actually constant even when very strict convergence criteria are applied.

In Fig. 5, the required total CPU time to satisfy the convergence criterion in the computed results is plotted in terms of the convergence criterion for $\delta = 40$. It can be seen that the reduction in the overall computational time is of the same order of magnitude

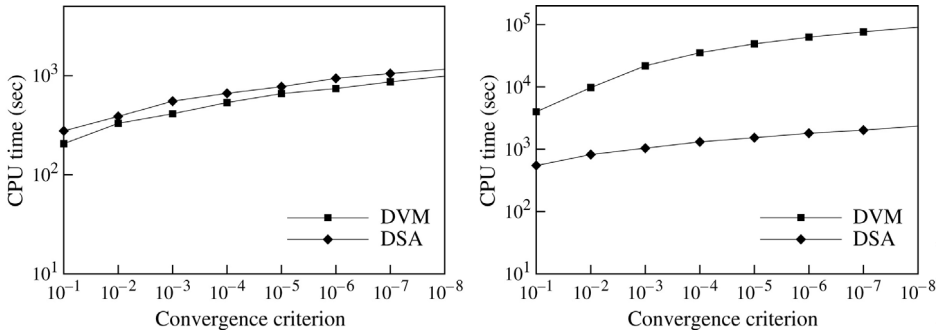

Fig. 5. Comparison between the DVM and the DSA method in terms of the required CPU time to satisfy the convergence criterion for $\delta = 1$ (left) and $\delta = 40$ (right).

with the reduction in the required number of iterations. This is easily explained by the fact that the additional computational effort per iteration is insignificant compared to the computational gain due to the small number of iterations required. The results have been obtained on a 2100 MHz, Athlon XP.

Overall, it is clearly seen that the number of required iterations is significantly reduced when the accelerated scheme is applied and this improvement becomes more important for small Knudsen numbers. Even more, in this case the typical DVM results suffer from accumulated round-off error due to the large number of iterations required and thus more strict convergence criteria does not always assure more accurate results. In general, when the DSA accelerated scheme is introduced we expect that the computational effort is reduced, while the accuracy of the results is improved.

6. Conclusions

The 2D flow problem of a gas mixture through a rectangular micro channel due to a small pressure gradient has been solved based on a mesoscopic approach. Numerical results for the flow rates and velocity profiles are presented for three different gaseous mixtures. Although the formulation is based on kinetic model equations the scheme is very efficient in terms of computational effort and time and accurate results are obtained for a wide range of Kn numbers. This is achieved by introducing a novel diffusion acceleration (DSA) scheme to speed up the very slow convergence rate of the discrete velocity method (DVM) near the hydrodynamic regime.

The proposed approach may be successfully implemented as an alternative, compared to other classical methods (finite volumes or elements), for simulation of gas flows where the continuum hypothesis breaks down as it happens in many occasions, in microfluidics and MEMS applications. In addition, the present work can be used for the estimation of the slip coefficients, which are commonly used in order to provide suitable boundary conditions for the Navier–Stokes equations in the slip regime. Recent work in that direction has shown that a detailed calculation of the slip coefficients, based on advanced kinetic theory approaches, may extend significantly the range of gas rarefaction, where the hydrodynamic equations can be applied.

Acknowledgements

The present research work has been partially supported by the Association EURATOM-Hellenic Republic (Contract ERB 5005 CT 990100) and the Conselho Nacional de Desenvolvimento Cientifico e Tecnologico (CNPq, Brazil).

Appendix. Elements of the McCormack collision term

The collision frequencies $\gamma_{\alpha\beta}$ are proportional to the collision frequency between the species α and β and they appear only in the combinations $\gamma_1 = \gamma_{11} + \gamma_{12}$ and $\gamma_2 = \gamma_{21} + \gamma_{22}$, where

$$\gamma_\alpha = \frac{S_\alpha S_\beta - \nu_{\alpha\beta}^{(4)} \nu_{\beta\alpha}^{(4)}}{S_\beta + \nu_{\alpha\beta}^{(4)}}$$

and

$$S_\alpha = \nu_{\alpha\alpha}^{(3)} - \nu_{\alpha\alpha}^{(4)} + \nu_{\alpha\beta}^{(3)}.$$

In the above equations $\alpha = 1, 2$ and $\alpha \neq \beta$. In addition

$$\nu_{\alpha\beta}^{(1)} = \frac{16}{3} \frac{m_{\alpha\beta}}{m_\alpha} n_\beta \Omega_{\alpha\beta}^{11}$$

$$\nu_{\alpha\beta}^{(2)} = \frac{64}{15} \left(\frac{m_{\alpha\beta}}{m_\alpha} \right)^2 n_\beta \left(\Omega_{\alpha\beta}^{12} - \frac{5}{2} \Omega_{\alpha\beta}^{22} \right)$$

$$\nu_{\alpha\beta}^{(3)} = \frac{16}{5} \frac{m_{\alpha\beta}^2}{m_\alpha m_\beta} n_\beta \left(\frac{10}{3} \Omega_{\alpha\beta}^{11} + \frac{m_\beta}{m_\alpha} \Omega_{\alpha\beta}^{22} \right)$$

$$\nu_{\alpha\beta}^{(4)} = \frac{16}{5} \frac{m_{\alpha\beta}^2}{m_\alpha m_\beta} n_\beta \left(\frac{10}{3} \Omega_{\alpha\beta}^{11} - \Omega_{\alpha\beta}^{22} \right)$$

$$\nu_{\alpha\beta}^{(5)} = \frac{64}{15} \left(\frac{m_{\alpha\beta}}{m_\alpha} \right)^3 \frac{m_\alpha}{m_\beta} n_\beta \left[\Omega_{\alpha\beta}^{22} + \left(\frac{15 m_\alpha}{4 m_\beta} + \frac{25 m_\beta}{8 m_\alpha} \right) \Omega_{\alpha\beta}^{11} - \frac{1}{2} \frac{m_\beta}{m_\alpha} (5 \Omega_{\alpha\beta}^{12} - \Omega_{\alpha\beta}^{13}) \right]$$

$$\nu_{\alpha\beta}^{(6)} = \frac{64}{15} \left(\frac{m_{\alpha\beta}}{m_\alpha} \right)^3 \left(\frac{m_\alpha}{m_\beta} \right)^{3/2} n_\beta \left[-\Omega_{\alpha\beta}^{22} + \frac{55}{8} \Omega_{\alpha\beta}^{11} - \frac{5}{2} \Omega_{\alpha\beta}^{12} + \frac{1}{2} \Omega_{\alpha\beta}^{13} \right]$$

and

$$m_{\alpha\beta} = \frac{m_\alpha m_\beta}{m_\alpha + m_\beta}.$$

Finally, the $\Omega_{\alpha\beta}^{ij}$ are the Chapman–Cowling integrals [24], which for the rigid sphere interaction read

$$\Omega_{\alpha\beta}^{ij} = \frac{(j+1)!}{2} \left[1 - \frac{1 + (-1)^i}{2(i+1)} \right] \left(\frac{\pi k T}{2 m_{\alpha\beta}} \right)^{1/2} (r_\alpha + r_\beta)^2$$

where r_α and r_β are the particle radius.

References

[1] C.M. Ho, Y.C. Tai, Micro-electro-mechanical systems (MEMS) and fluid flows, Annu. Rev. Fluid Mech. 30 (1998) 579.
[2] C. Cercignani, The Boltzmann Equation and its Applications, Springer-Verlag, 1988.
[3] A. Beskok, G.E. Karniadakis, W. Trimmer, Rarefaction and compressibility effects in gas micro-flows, J. Fluid Eng. 118 (1996) 448.
[4] E.P. Muntz, Rarefied gas dynamics, Annu. Rev. Fluid Mech. 21 (1989) 387.
[5] G.A. Bird, Molecular Gas Dynamics and the Direct Simulation of Gas Flows, Oxford University Press, 1996.
[6] S. Succi, The Lattice Boltzmann Equation for Fluid Dynamics and Beyond, Oxford University Press, 2001.
[7] F. Sharipov, V. Seleznev, Data on internal gas flows, J. Phys. Chem. Ref. Data 27 (3) (1998) 657.
[8] F. Sharipov, Non-isothermal gas flow through rectangular micro-channels, J. Micromech. Microeng. 9 (1999) 394.
[9] D. Valougeorgis, S. Naris, Acceleration schemes of the discrete velocity method: gaseous flows in rectangular microchannels, SIAM J. Sci. Comput. 25 (2) (2003) 534.
[10] S.K. Loyalka, Temperature jump in a gas mixture, Phys. Fluids 17 (1974) 897.
[11] D. Valougeorgis, Couette flow of a binary gas mixture, Phys. Fluids 31 (1988) 521.
[12] I.N. Ivchenko, S.K. Loyalka, R.V. Tompson, Slip coefficients for binary gas mixtures, J. Vac. Sci. Technol. A 15 (4) (1996) 2375.
[13] C.E. Siewert, Couette flow for a binary gas mixture, J. Quant. Spectrosc. Radiat. Transf. 70 (2001) 321.
[14] F. Sharipov, D. Kalempa, Gaseous mixture flow through a long tube at arbitrary Knudsen numbers, J. Vac. Sci. Technol. A 20 (3) (2002) 814.
[15] C.E. Siewert, D. Valougeorgis, Concise and accurate solutions to half-space binary-gas flow problems defined by the McCormack model and specular-diffuse wall conditions, Eur. J. Mech. B/Fluids (in press).
[16] S. Naris, D. Valougeorgis, D. Kalempa, F. Sharipov, Gaseous mixture flow between parallel plates in the whole range of rarefaction, Physica A 336 (2004) 249.
[17] F.J. McCormack, Construction of linearized kinetic models for gaseous mixtures and molecular gases, Phys. Fluids 16 (12) (1973) 2095.
[18] F.M. Sharipov, E.A. Subbotin, On optimization of the discrete velocity method used in rarefied gas dynamics, Z. Angew. Math. Phys. 44 (1993) 572.
[19] M.L. Adams, E.W. Larsen, Fast iterative methods for discrete-ordinates particle calculations, Prog. Nucl. Energy 40 (2002) 3.
[20] S.K. Loyalka, T.S. Storvick, Kinetic theory of thermal transpiration and mechanocaloric effect. III. Flow of a polyatomic gas between parallel plates, J. Chem. Phys. 71 (1979) 339.
[21] E.E. Lewis, W.F. Miller Jr., Computational Methods of Neutron Transport Theory, Wiley, New York, 1984.
[22] F. Sharipov, D. Kalempa, Velocity slip and temperature jump coefficients for gaseous mixtures. I. Viscous slip coefficient, Phys. Fluids 15 (2003) 1800.
[23] J. Kestin, K. Knierim, E.A. Mason, B. Najafi, S.T. Ro, M. Waldman, Equilibrium and transport properties of the noble gases and their mixture at low densities, J. Phys. Chem. Ref. Data 13 (1984) 229.
[24] J.H. Ferziger, H.G. Kaper, Mathematical Theory of Transport Processes in Gases, North-Holland Publishing Company, Amsterdam, 1972.